Journal of Industrial Microbiology & Biotechnology (2000) 24, 146–151

www.nature.com/jim

Effect of pH on the biosorption of nickel and other heavy metals by *Pseudomonas fluorescens* 4F39

A López, N Lázaro, JM Priego and AM Marqués

Laboratori de Microbiologia, Department de Microbiologia i Parsitologia Sanitàries, Universitat de Barcelona, Barcelona, Spain

Accumulation of heavy metals by *Pseudomonas fluorescens* 4F39 was rapid and pH-dependent. The affinity series for bacterial accumulation of metal cations decreased in the order Ni>>Hg>U>>As>Cu>Cd>Co>Cr>Pb. Metal cations were grouped into those whose accumulation increased as the pH increased, with a maximum accumulation at the pH before precipitation (Ni, Cu, Pb, Cd, Co), and those whose maximum accumulation was not associated with precipitation (Cr, As, U, Hg). High Ni^{2+} accumulation was studied. Electron microscopy indicated that at pH 9, Ni^{2+} accumulated on the cell surface as needle and hexagon-like precipitates, whose crystalline structure was confirmed by electron diffraction analysis and corresponded to two different orientations of the nickel hydroxide crystals. Crystals on cells showed marked anisotropy by X-ray powder diffraction, which differentiated them from crystals observed in nickel solution at pH 10 and 11 and from commercial nickel hydroxide. Nickel biosorption by *Pseudomonas fluorescens* 4F39 was a microprecipitation consequence of an ion exchange. *Journal of Industrial Microbiology & Biotechnology* (2000) **24,** 146–151.

Keywords: nickel; heavy metals; biosorption; pH; accumulation

Introduction

Domestic activities and especially industrialization have accelerated the geochemical cycling of heavy metals. Consequently, if sewage is not treated correctly, it can carry metals in solution, which eventually reach surface waters or the sea [4]. In recent years, attention has been focused on the use of microorganisms for removal and possible recovery of metal ions and radionuclides from industrial wastes. This is a potential alternative to existing technologies (chemical precipitation, reverse osmosis, solvent extraction), which have significant disadvantages, such as high chemical or energy requirements and generation of toxic sludge or other products that need disposal [5]. The complexity of the structure of microorganisms implies that there may be many mechanisms associated with metal accumulation, some of which are still not well elucidated, but its application potential is obvious and intriguing [23].

It is important to distinguish two types of metal accumulation by microorganisms. First, bioaccumulation, an active mode of metal accumulation is dependent on the metabolic activity of the cell, which, in turn can be affected significantly by the presence of metallic ions. Bioaccumulation requires time for uptake by the microorganism [19,21]. In contrast, biosorption is relatively rapid and can be reversible. It involves a physicochemical interaction between the metal and functional groups on the cell surface, based on physical adsorption, ion exchange, complexation, and precipitation [18]. Metal biosorption performance depends on external factors, such as pH, other ions in solution (which may be in competition), organic material in solution (such as complexing agents), cell metabolic products in solution (which may cause metal precipitation), and temperature [20]. The development of biosorption may provide a basis for a technology aimed at the removal of heavy metal species from dilute solutions [21].

Correspondence: AM Marques, Laboratori de Microbiologia, Facultat de Farmàcia, Av Joan XXIII s/n, 08028 Barcelona, Spain. E-mail: amarques@far.ub.es
Received 22 June 1999; accepted 4 December 1999

Materials and methods

Microorganism

Pseudomonas fluorescens strain 4F39 was isolated from sludge samples from the wastewater treatment plant of an electroplating plant in Barcelona (Spain). The sludge was vigorously suspended in sterile distilled water and passed through filter paper to remove inert particles. Bacterial colonies were isolated from the filtrate on Mueller–Hinton agar. Strains were maintained on the isolation medium. Strain 4F39 was selected for its high capacity of nickel accumulation and was identified as *P. fluorescens* by traditional methods [10].

Accumulation experiments

For accumulation experiments, *P. fluorescens* 4F39 was grown on a medium containing (per liter of water): 20 g peptone protease; 1.5 g glycerol; 1.5 g K_2SO_4 and 1.5 g $MgSO_4 \cdot 7H_2O$ [17]. The pH was adjusted to 7 with NaOH. After 48 h of incubation, cells were harvested by centrifugation and washed twice with water. Metal accumulation experiments were carried out at 30°C in shaker flasks containing 40 ml of metal solution, so that the addition of 10 ml of a cell suspension provided the appropriate dilution to give the desired initial metal concentration (0.85 mM) and cell density (0.4 mg dry weight ml^{-1}). The initial pH of the metal solution was adjusted with 0.1 N NaOH or 0.1 N HCl. $NiCl_2$, $CdCl_2$, $HgCl_2$, $Pb(NO_3)_2$, $CoCl_2$,

Na_2HAsO_4, K_2CrO_4, $CuSO_4$ and $UO_2(NO_3)_2$ were used. Samples (5 ml) were removed for metal determination after 5 min, 30 min, 1 h, and 24 h. The amount of metal accumulated by the biomass was determined by measuring the residual metal concentration in the supernatant after centrifugation, using a Philips PU 9200× atomic absorption spectrophotometer (AAS, UK). All experimental results were expressed as the mean of analysis from three replicate flasks. Controls without cells, treated in the same way, were done at each pH as a control for precipitation. Dry weight of bacterial cells was obtained by drying a measured volume at 105°C to constant weight.

Electron microscopy

Nickel-exposed cells were fixed for 2 h at 4°C in 1% glutaraldehyde, washed three times with distilled water, dehydrated though a graded series of acetone solutions, and embedded in Spurr resin. Ultrathin sections (<0.1 μm) were cut with a Reichert–Jung Ultracut microtome (Wien, Austria) and mounted on 200-mesh copper grids. Unstained thin sections were examined without further processing in a Phillips EM 301 transmission electron microscope (TEM, Eindhoven, Netherlands) at 80 kV. Control cells were treated in the same way, but they were lightly stained with 2% uranyl acetate and lead citrate for 10 min to provide better visualization.

Energy dispersive X-ray microanalysis and electron diffraction

Thick sections of cells (0.5 μm) were mounted on 200-mesh titanium grids. Electron-dense structures were analyzed using a Philips CM 30/STEM (300 kV) electron microscope equiped with a Link model LZ5 energy dispersive X-ray spectrophotometer (Eindhoven, Netherlands).

Crystal structure by X-ray powder diffraction (XRD)

The crystal structure of precipitates of nickel on cells was determined by X-ray powder diffraction of cells (from Ni solutions at pH 9) and metal solutions at pH 9, 10, 11 and, 12. After 1 h of contact with nickel, cells were recovered by centrifugation, and organic matter was removed by adding 30% H_2O_2 in increments of 5 ml to cells suspended in distilled water (1:1) until the sample ceased to froth. It was then transferred to a steam bath (65–70°C) until any strong reaction was complete. The sample was centrifuged, and the pellet was dried [12]. Nickel solutions received the same treatment. X-ray powder diffraction measurements were performed in a Bragg Brentano diffractometer Siemens D-500 (Karlsruhe, Germany) ($\theta/2\theta$) using CuKα radiation, at 40 kV and 30 mA ($\lambda = 0.15418$ nm), selected with a graphite secondary monochromator. Power diffraction patterns were recorded from 4–70° (2θ) with a step size of 0.05° (2θ) and a measuring time of 3 s step^{-1}.

Results

The metal accumulation properties of *P. fluorescens* 4F39 were measured as metal removal from aqueous solution by nongrowing biomass at different pH values. As industrial wastewater can be contaminated with more than one heavy metal, we examined whether strain 4F39 was able to take up nine metals separately at equimolar concentrations.

The initial pH of the solution had a marked effect on accumulation of Ni by cells. The accumulation was 130 μmol Ni g^{-1} dry weight (0.75%) after 1 h of contact at pH 7 (Figure 1a). When the pH was raised to 9, accumulation of Ni increased markedly to 1700 μmol Ni g^{-1} dry weight (10%) (Figure 1a). Control flasks at pH 9 showed 3.2% precipitation. At pH 11, the metal precipitated (86%). At pH 9 (optimum), metal accumulation was extremely rapid; the maximum amount of Ni was removed from solution by bacterial biomass in 5 min (time required for sample manipulation) and remained constant for 24 h.

Accumulation of metals was studied using a pH up to 5 for Cu and Pb or up to 7 for Cd and Co, as at higher pH values, these metals precipitated. Accumulation of Cr, As, U, and Hg was studied using a pH up to 11. In addition to Ni, *P. fluorescens* 4F39 adsorbed other heavy metals. Uptake after 1 h (at the optimum pH) was high for Hg and U (880 and 710 μmol g^{-1} dry weight respectively) (Figure 1b and c); medium for As, Cu, and Cd (420, 270, and 245 μmol g^{-1} dry weight respectively) (Figure 1d, e, f); and lower for Co, Cr and Pb (216, 160, and 115 μmol g^{-1} dry weight respectively) (Figure 1g, h, i). The metals were divided into two groups according to the effect of pH: (i) those whose accumulation increased with an increase in pH. The maximum accumulation occurred before pH-induced precipitation. This group included Ni, Cu, Pb, Cd, and Co; (ii) those whose maximum accumulation was not associated with the pH of precipitation. This group included Cr, As, U, and Hg. The oxoanions, CrO_4^{-2} and AsO_4^{-3}, need a pH $\leqslant 3$ for optimum accumulation. The optimum pH for accumulation of U was 5. The microorganism accumulated a large amount of Hg (Figure 1b). The amount of Hg taken up was determined in both the supernatant and the pellet (data not shown), confirming that the decrease in the concentration of Hg in the supernatant was a consequence of cellular accumulation and not reduction to Hg° and volatilization.

The kinetics of accumulation of each metal were studied at the pH of optimum accumulation, and found to be similar to that of Ni. The maximum amount of metal was accumulated by bacterial biomass in about 5 min. The amount of metal accumulated doubled after 24 h only for Cu and Hg. Further studies are required to determine whether this accumulation is metabolism-dependent or is a nonspecific accumulation as a consequence of nucleation point-sites that increase the amount of metal precipitated on the bacterial surface.

The high accumulation of Ni at pH 9 was studied. Cells of *P. fluorescens* 4F39 exposed to Ni (pH 9, 1 h and 24 h) were examined by TEM. All cells showed two electron-dense structures associated with the cellular envelope (Figure 2d and e): needle-like fibrils (highly electron-dense), approximately 2.4 nm thick (Figure 2a), and hexagon-like crystals (low electron-dense), approximately 56 nm × 41 nm (Figure 2b). Some of these cells had even larger precipitates (Figure 2e), which resembled a loose, crystalline collection of two electron-dense structures of Ni; it seemed that the small precipitates were nucleated at distinct sites on the outer membrane and that they grew, over

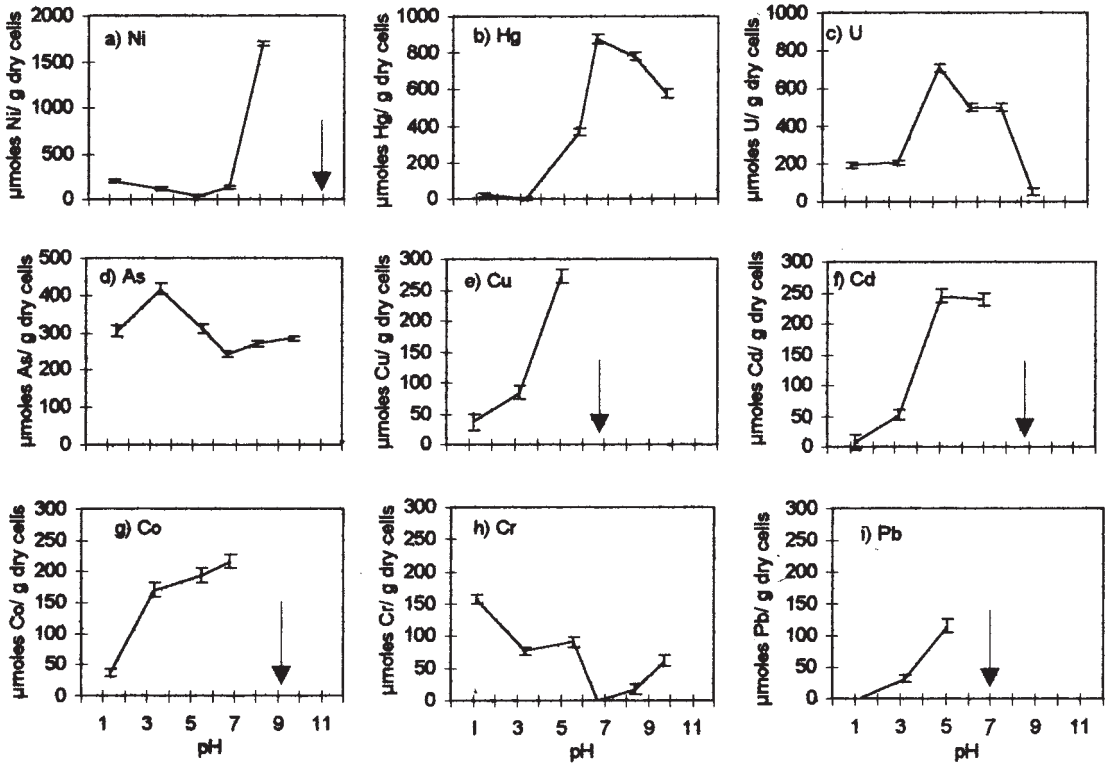

Figure 1 Metal accumulation at pH of equilibrium, after 1 h contact with 0.85 mM of: (a) Ni^{2+}; (b) Hg^{2+}; (c) UO_2^{2+}; (d) AsO_4^{3-}; (e) Cu^{2+}; (f) Cd^{2+}; (g) Co^{2+}; (h) CrO_4^{2-}; and (i) Pb^{2+}. ↓: metal precipitation at and above this pH. Bars indicate standard deviation.

time (24-h samples), into larger aggregates. These structures were not observed in control cells (Figure 2c).

Energy X-ray microanalysis, used to confirm the identity of the electron-dense structures on the cells, revealed the presence of Ti, from the grid, Cl, Si, and P, as expected for biological material, and Ni (Figure 3). Identical spectra were obtained for the two structures (needle and hexagon-like). The observation of electron-dense structures in the bacteria by electron diffraction analysis showed a spot-like ring pattern, indicating that the precipitate was crystalline.

XRD analysis of the precipitate present on cells revealed an unusual pattern (Figure 4), consisting of a high narrow peak and a lower broader peak, both of which corresponded to $Ni(OH)_2$. This pattern indicated anisotropy of form, in which the same crystal showed two orientations. $NiCl_2$ was not detected. Commercial $Ni(OH)_2$ (Fluka, Buchs, Switzerland) also showed two peaks (Figure 4), but they were more homogeneous. Two types of crystal can be differentiated on the basis of these results. One type was formed at pH 9 in the presence of *P. fluorescens* 4F39 with more marked anisotropy of form, and the other was formed from the commercial product.

XRD analysis of the Ni solution at pH 9, 10, and 11 showed the presence of NaCl in crystalline form as a result of the reaction of Na^+ from NaOH added to adjust the pH and Cl^- from $NiCl_2$. At pH 9 the pH decreased to 8 after a few minutes and only traces of crystalline $Ni(OH)_2$ were detected, corresponding to 3% precipitation detected by atomic absorption spectroscopy of the control solution. At pH 10 (Figure 5) and pH 11 metal precipitation was evident and $Ni(OH)_2$ was also detected, but it was different from that formed in the presence of cells at pH 9. At pH 12, crystalline Ni species were not detected. These results suggest that the presence of different crystalline $Ni(OH)_2$ at pH 9 was a consequence of the presence of *P. fluorescens* 4F39 cells.

Discussion

The ability of microorganisms to accumulate heavy metals suggests they could be used to decontaminate wastewater polluted with dissolved metals. The accumulation of metals on the surface of microbial cells is a consequence of the net negatively-charged surface [13] and is influenced by the chemistry of the cell wall, physicochemical characteristics of the environment, such as pH, and the sequence of metal hydrolysis.

The cell wall contains amines, amides, and carboxylic functional groups that are protonated or deprotonated, depending on the pH of the aqueous medium [9]. Increasing the pH increases the negative charge at the surface of the cells until all relevant functional groups are deprotonated, which favours electrochemical attraction and adsorption of cations. Furthermore, the increase in metal uptake with an increase in pH may be the result of more efficient competition of cations with H^+ for binding sites on bacteria. Anions could be expected to interact more strongly with cells as the concentration of positive charges increases, as the result of protonation of functional groups at low pH values [3].

Metal ions in solution undergo hydrolysis as the pH increases. The extent of hydrolysis at different pH values

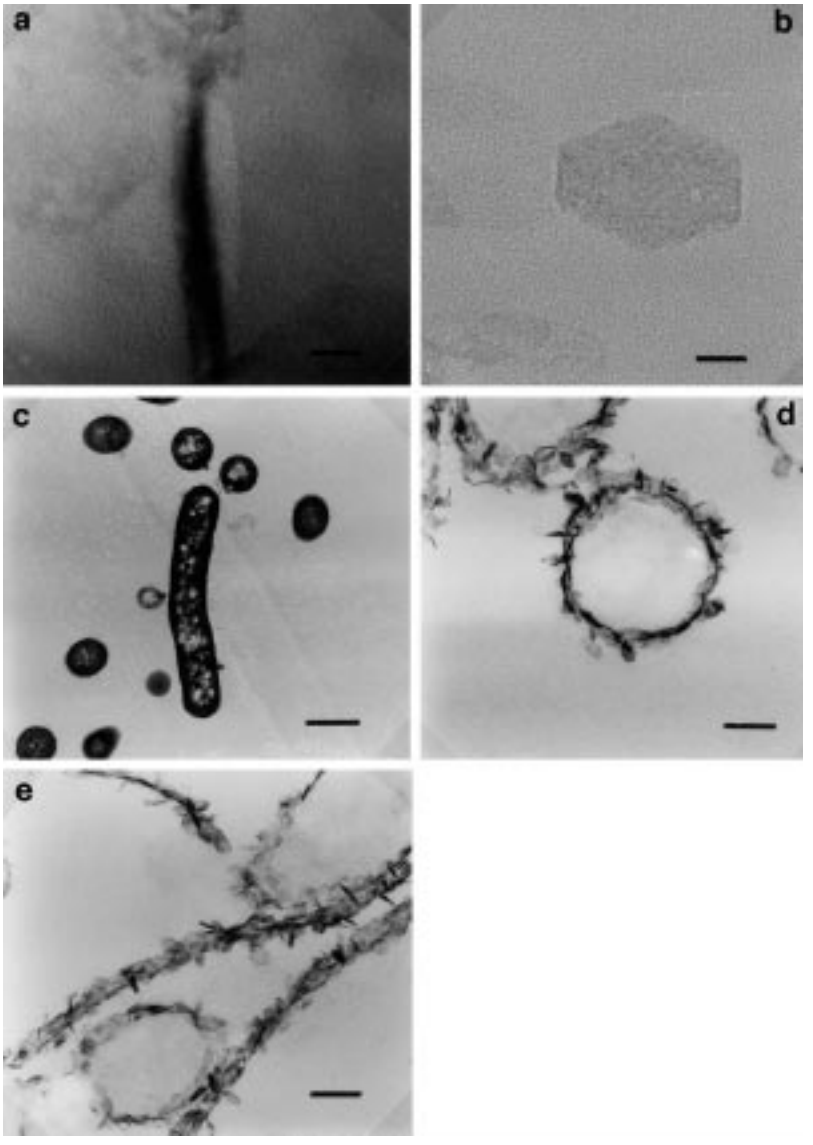

Figure 2 Transmission electron micrographs. (a) Needle-like fibril, 2.4 nm thick. Bar = 7 nm. (b) Hexagon-like crystal, 56 nm × 41 nm. Bar = 16 nm. (c) Stained control cells without nickel. Bar = 0.45 μm. (d) *P. fluorescens* 4F39 cells after 1 h contact with nickel. Bar = 0.12 μm. (e) Cells after 24 h contact with nickel. Bar = 0.14 μm.

differs with each metal, but the usual sequence of hydrolysis is the formation of hydroxylated monomeric species followed by the formation of polymeric species, and then the formation of crystalline oxide precipitates after aging [2]. The different chemical species of a metal that occur with changes in pH vary in charge and adsorbability at solid–liquid interfaces. Therefore, adsorption of metals on interfaces is highly pH-dependent, and there is a critical pH range, usually of less than one pH unit, for each metal wherein the amount of metal adsorbed increases significantly [7,8].

The high accumulation of Ni by *P. fluorescens* 4F39 at pH 9 led us to study this process more thoroughly. At this pH, all cells in the population examined by TEM had accumulated significant amounts of two electron dense structures of Ni on their cell walls, corresponding to two orientations of crystals of $Ni(OH)_2$.

Studying the mechanism for metal ion binding to the biomass is complicated by the fact that metal cations are hydrolyzed in aqueous solutions within the pH range of the sorption system studied here. Partitioning of the hydrolysed metal species depends on the solution pH and on the total metal concentration in solution. The equilibrium composition calculations and formation constants have been carried out by the computer program SOL1 [11]. Chloride complexes formed as a consequence of 0.1 M HCl medium have also been taken into account.

In the range of pH 1–7, one major hydrolysed metal species, Ni^{2+} (90%), exists in the solution [1,11,15]. At pH 9 Ni^{2+} (68%), $Ni_4OH_4^{4+}$ (10%, log β = 28.3) and $Ni(OH)^+$ (8.6%, log β = 4.1) were predicted [11]. When the Ni solution was adjusted to pH 1–5 (no buffer was used to prevent interference in metal accumulation), a small increase in pH ($<$0.5 unit) was detected after 5–10 min. At pH 7, the pH was maintained, but when the $NiCl_2$ solution was adjusted to pH 9, the pH decreased to 8 after a few minutes.

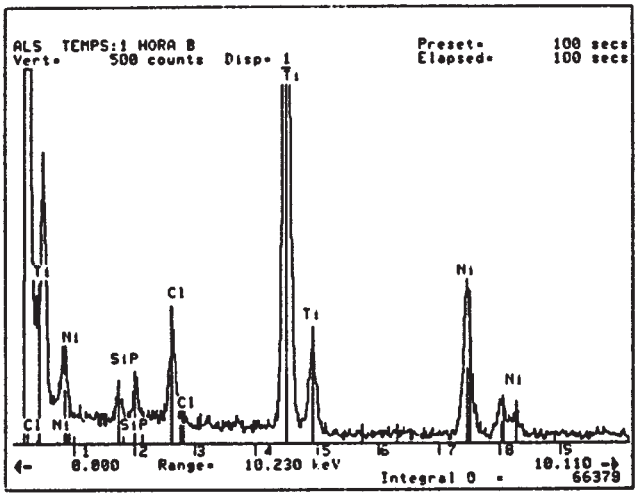

Figure 3 Energy-dispersive X-ray spectra obtained from cells after nickel accumulation. The titanium signal was assumed to be from the sample grid.

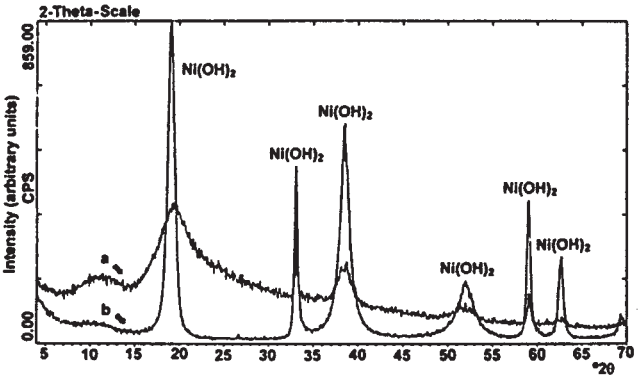

Figure 4 Analysis by X-ray powder diffraction of (a) the precipitate of nickel present on cells after metal accumulation at pH 9, and (b) commercial nickel hydroxide.

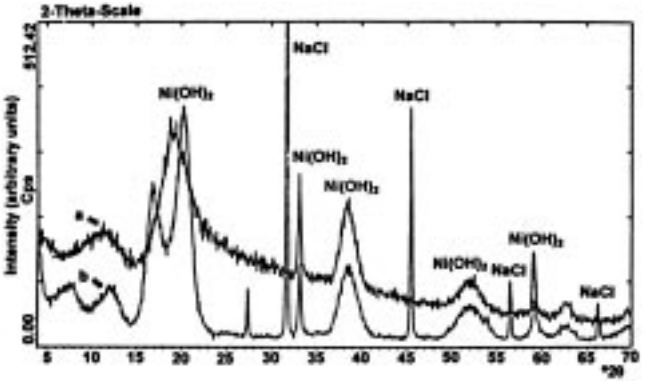

Figure 5 Analysis by X-ray powder diffraction of (a) the precipitate of nickel present on cells after metal accumulation at pH 9, and (b) the nickel precipitate in the metal solution at pH 10.

Based on atomic absorption measurements, the pH decrease of the metal solution was associated with a 3% decrease in nickel concentration in the supernatant as the result of metal precipitation.

When cells were added (0.4 mg dry weight ml^{-1} metal solution) to a solution of Ni at pH 1–5, the pH increased after a few minutes ($\leq$0.5 pH unit) as a consequence of the dilution made with the inoculum and the buffering power of cells [16]. When cells were added to a solution of Ni at pH 9, the pH decreased to 7.5 and a rapid decrease in Ni concentration in the medium was measured. This decrease was associated with microprecipitation of $Ni(OH)_2$ crystals on the bacterial surface. Ni accumulation increased when the initial pH was 9. According to the distribution of ionic species of Ni of the computer program SOL 1 [11], this increase corresponded to the appearance of hydroxylated species of Ni. Collins and Stotzky [7] described a charge reversal of bacteria with Ni at pH values above 7.0, as all cells became net positively charged, and most remained positively charged at pH values above 9.0. They considered that the ability of a metal to cause charge reversal is related to the speciation of the metal that occurs at different pH values and to the ability of some speciation forms to be specifically adsorbed on the cell surface. However, when Ni accumulation of *P. fluorescens* 4F39 was assayed at an initial pH of 7.5, metal accumulation was lower. The absence of hydroxylated species reduced the accumulation of the metal.

As with Ni^{2+}, the accumulation of Pb^{2+}, Co^{2+}, Cd^{2+} and Cu^{2+} increased as the pH increased, reaching a maximum below the pH at which precipitation occurred. As with solutions of Ni^{2+}, solutions of metals were not buffered and an increase of initial pH was observed in 5–10 min ($<$0.5 unit). At pH 1–5 the species of Pb and Cu were $PbCl^+$ (70%, log β = 1.6), Pb^{2+} (18%), $PbCl_2$ (11%, log β = 1.8), Cu^{2+} (80%), and $CuCl^+$ (20%, log β = 0.4) respectively [11]. As pH increased, accumulation increased since ion exchange is more effective when less H^+ is available to compete with the metal for negatively-charged metal-binding sites. With Cd and Co between pH 1 and pH 7, SOL 1 [11] predicted the same chemical species $CdCl^+$ (64%, log β = 1.9), $CdCl_2$ (27%, log β = 2.6) and, Co^{2+} (91%) respectively. Also with these species an increase of accumulation was present as the pH of the medium increased. Hydrolyzed metal cations accumulated as a consequence of ionic exchange with protons. Our accumulation results correlated with the charge reversal described by Collins and Stotzky [6,7], indicating a close binding of these metals on the surface of the cells.

Uranium tends to be accumulated well by microorganisms, including *P. fluorescens* 4F39, which may be related to its heavy atomic weight and ionic radius [22]. The hydrolysed U species for pH values below 5, in the conditions employed in this work were, according to the SOL1 program, UO^{2+} (86%) and UO_2Cl^+ (14%, log β = 0.2). At pH 5 the hydroxylated forms $(UO_2)_3(OH)_5^+$ (77%, log β = 54.4) and $(UO_2)_2(OH)_2^{2+}$ (11%, log β = 22.4) appeared which corresponded to a significant increase in uranium accumulation. As with Ni hydroxylated uranyl ions have a higher binding capacity on the biomass. The speciation form of the metal appeared to be an important factor in determining metal accumulation. In contrast to the metals previously mentioned, U did not precipitate when the pH was alkaline. With non-buffered metal solutions at pH 9 and 11 more instability was observed and a decrease of 1–1.5 units of pH at pH 11 or 1–0.5 units of pH at pH

9 were observed 5–10 min after the addition of inoculum. At pH 7 and above, $(UO_2)_3(OH)_5^-$ (99%) predominated in solution and a decrease in accumulation of U was observed.

According to SOL1 [11] the species of Hg predicted between pH 1 and pH 7 were negatively charged and uncharged chlorinated species ($HgCl_2$ 40%, log β = 13.2; $HgCl_3^-$ 30%, log β = 14.1; and $HgCl_4^{2-}$ 30%, log β = 15.1), and at acidic pH a high accumulation could be expected as a consequence of electrostatic binding to positively charged groups. Nevertheless, a high accumulation was observed at pH 7 and alkaline pH. A qualitative reason has been suggested to explain why the chlorinated forms of Hg were adsorbed more at pH 7 or alkaline pH than at acidic pH. Hg^{2+} is a 'soft' cation and complexes strongly with numerous ligands, a consequence of its strong affinity for sulfur-donating ligands and halogens [2]. Soft ions participate in covalent binding with ligands and electrostatic binding is relatively unimportant [6,14]. Additionally, covalent binding is affected minimally by ionic interactions and pH [3]. Complexation could be the mechanism responsible for metal accumulation, especially at alkaline pH. The high accumulation of Hg and U at alkaline pH could be a consequence of metal complexation.

AsO_4^{3-} and, especially, CrO_4^{2-} bound more strongly to *P. fluorescens* 4F39 at acidic pH. As the pH decreased below the isoelectric pH, the overall net positive charge on the cell wall promoted an easier access of anions ($AsO_4H_2^-$ 85%, log β = 18.4 at pH 3 or $HCrO_4^-$ 83%, log β = 6.5 at pH 1) to positively charged binding sites. At low pH, the accumulation of these oxoanions was consistent with electrostatic binding to positively charged groups.

Until recently, attention has been focused principally on cation adsorption or ion exchange processes on the cell wall. Ion exchange has been considered the main mechanism responsible for metal accumulation. Metal precipitation and metal nucleation, which play a special role in the metal deposition process, are also important. However, other mechanisms such as complexation, coordination or chelation can contribute to metal sequestration on or in the cell walls.

pH is the most important factor in the metal-accumulation process; it affects the solution chemistry of the metals, the activity of functional groups in the biomass, and competition between metallic ions. The accumulation of Ni by *P fluorescens* 4F39 was the result of a combined ion exchange-microprecipitation mechanism on the cell surface, and it can be considered a biosorption process. This property may lead to applications that could contribute to the process of metal immobilization.

Acknowledgements

We thank Serveis Cientifico-Tècnics de la Universitat de Barcelona for technical assistance. This work was supported by a grant from Departament del Medi Ambient, Direcció General de Qualitat Ambiental, Generalitat de Catalunya. The work was carried out under The II Pla de Recerca de Catalunya No. expedient 1997SGR 00473. We are grateful to Josep Lluis Beltran for help and expert criticism during preparation of this manuscript.

References

1 Babich H and G Stotzky. 1983. Toxicity of nickel to microbes: environmental aspects. In: Advances in Applied Microbiology (Laskin Al, ed), pp 195–265, Academic Press, New York.
2 Baes CF and RE Mesmer. 1976. The Hydrolysis of Cations. pp 241–310, John Wiley & Sons, New York.
3 Bedell GW and DW Darnall. 1990. Immobilization of nonviable, biosorbent, algal biomass for the recovery of metal ions. In: Biosorption of Heavy Metals (Volesky B, ed), pp 313–326, CRC Press, Boca Raton, FL.
4 Bordons A and J Jofre. 1987. Extracellular adsorption of nickel by a strain of *Pseudomonas* sp. Enzyme Microb Technol 9: 709–713.
5 Bossrez S, J Remacle and J Coyette. 1997. Adsorption of nickel on *Enterococcus hirae* cell walls. J Chem Tech Biotechnol 70: 45–50.
6 Collins YE and G Stotzky. 1989. Factors affecting the toxicity of heavy metals to microbes. In: Metals lons and Bacteria (Beveridge TJ and RJ Doyle, eds), pp 31–90, John Wiley and Sons, New York.
7 Collins YE and G Stotzky. 1992. Heavy metals alter the electrokinetic properties of bacteria, yeast, and clay minerals. Appl Environ Microbiol 58: 1592–1600.
8 Collins YE and G Stotzky. 1996. Changes in the surface charge of bacteria caused by heavy metals do not affect survival. Can J Microbiol 42: 621–627.
9 Guibal E, C Roulph and P Le Cloirec. 1992. Uranium biosorption by a filamentous fungus *Mucor miehei*; pH effect on mechanisms and performances of uptake. Water Res 26: 1139–1145.
10 Holt JG, NR Krieg, PHA Sneath, JT Staley and St Williams. 1994. Bergey's Manual of Determinative Bacteriology, 9th edn, pp 141–218, Williams and Wilkins, Baltimore.
11 Izquierdo A and JL Beltran. 1988. SOL 1: a program for the simulation of complex equilibria using a personal computer. J Chemometrics 3: 209–216.
12 Kunze GW and SB Dixon. 1986. Pretreatment for mineralogical analysis. In: Methods of Soil Analysis. Part 1. Physical and Mineralogical Methods (Klute A, ed), pp 91–100. American Society of Agronomy, Wisconsin, USA.
13 Langley S and TJ Beveridge. 1999. Effect of O-side-chain-lipopolysaccharide chemistry on metal binding. Appl Environ Microbiol 65: 489–498.
14 Remacle J. 1990. The cell wall and metal binding. In: Biosorption of Heavy Metals (Volesky B, ed), pp 83–92, CRC Press, Boca Raton, FL.
15 Richter RO and TL Theis. 1980. Nickel speciation in a soil/water system. In: Nickel in the Environment (Nriagu JO, ed), pp 189–202, John Wiley & Sons, New York.
16 Rius N, M Solé and JG Lorén. 1998. Acid-base response of bacterial suspensions. J Ind Microbiol & Biotechnol 21: 65–74.
17 Stolp H and D Gadkari. 1981. Nonpathogenic members of the genus *Pseudomonas*. In: The Prokaryotes. A Handbook on Habitats, Isolation and Identification of Bacteria, Vol 1 (Starr MP, Stolp H, Trüper HG, Ballows A and Schlegel HG, eds), pp 719–741, Springer Verlag, Berlin.
18 Tsezos M, E Remoudaki and V Angelatou. 1996. A study of the effects of competing ions on the biosorption of metals. Int Biodeter Biodegrad 38: 19–29.
19 Veglio' F and F Beolchini. 1997. Removal of metals by biosorption: a review. Hydrometallurgy 44: 301–316.
20 Veglio' F, F Beolchini and A Gasbarro. 1997. Biosorption of toxic metals: an equilibrium study using free cells of *Arthrobacter* sp. Process Biochem 32: 99–105.
21 Volesky B. 1990. Biosorption and biosorbents. In: Biosorption of Heavy Metals (Volesky B, ed), pp 3–5, CRC Press, Boca Raton, FL.
22 Volesky B. 1994. Advances in biosorption of metals: selection of biomass types. FEMS Microbiol Rev 14: 291–302.
23 Volesky B and I Prasetyo. 1994. Cadmium removal in a biosorption column. Biotechnol Bioeng 43: 1010–1015.